# Targeting Ornithine Decarboxylase Impairs Development of *MYCN*-Amplified Neuroblastoma

**Robert J. Rounbehler, Weimin Li, Mark A. Hall, Chunying Yang, Mohammad Fallahi, and John L. Cleveland**

Department of Cancer Biology, The Scripps Research Institute, Scripps Florida, Jupiter, Florida

## Abstract

**Neuroblastoma is a pediatric malignancy that arises from the neural crest, and patients with high-risk neuroblastoma, which typically harbor amplifications of *MYCN*, have an extremely poor prognosis. The *tyrosine hydroxylase* (TH) promoter-driven TH-*MYCN* transgenic mouse model faithfully recapitulates many hallmarks of human *MYCN*-amplified neuroblastoma. A key downstream target of Myc oncoproteins in tumorigenesis is *ornithine decarboxylase* (*Odc*), the rate-limiting enzyme of polyamine biosynthesis. Indeed, sustained treatment with the Odc suicide inhibitor α-difluoromethylornithine (DFMO) or *Odc* heterozygosity markedly impairs lymphoma development in Eμ-*Myc* transgenic mice, and these effects are linked to the induction of the cyclin-dependent kinase (Cdk) inhibitor $p27^{Kip1}$, which is normally repressed by Myc. Here, we report that DFMO treatment, but not *Odc* heterozygosity, impairs *MYCN*-induced neuroblastoma and that, in this malignancy, transient DFMO treatment is sufficient to confer protection. The selective anticancer effects of DFMO on mouse and human *MYCN*-amplified neuroblastoma also rely on its ability to disable the proliferative response of Myc, yet in this tumor context, DFMO targets the expression of the $p21^{Cip1}$ Cdk inhibitor, which is also suppressed by Myc oncoproteins. These findings suggest that agents, such as DFMO, that target the polyamine pathway may show efficacy in high-risk, *MYCN*-amplified neuroblastoma.** [Cancer Res 2009;69(2):547–53]

## Introduction

Neuroblastoma is a childhood malignancy that accounts for nearly 8% of all childhood cancers and 15% of pediatric cancer–related deaths (1). This tumor arises from sympathetic nervous tissue, most commonly in the adrenal gland, and its onset is age-dependent, with an incidence, during the first year of life, twice that of the second. Furthermore, neuroblastoma is the most common cancer during infancy, with an incidence nearly twice that of pediatric leukemia. Tragically, children with stage IV, high-risk neuroblastoma have a <40% long-term survival (2).

The best-described genetic alteration in neuroblastoma is the amplification of the proto-oncogene *MYCN*, which occurs in ~20% of all neuroblastoma and is associated with the high-risk phenotype (3, 4). *MYCN* is a member of the *Myc* family of transcription factors, which function as master regulators that coordinate cell growth (mass), cell metabolism, and division and which are activated in up to 70% of rapidly dividing malignancies. Their selective activation in cancer likely reflects their regulation of a large cast of genes involved in cell metabolism and proliferation, as well as in tumor angiogenesis and metastasis (5). Indeed, expression profiling and genome-wide chromatin binding analyses suggest that Myc can regulate the transcription of up to 15% of the genome (6, 7). Enforced expression of Myc in transgenic mouse models is sufficient to provoke a wide array of malignancies that accurately phenocopy human malignancies (8–11). This is particularly true of the *tyrosine hydroxylase* (TH) promoter-driven expression of N-Myc in neural crest progenitors that gives rise to a malignancy that faithfully recapitulates *MYCN*-amplified stage IV neuroblastoma, including shared syntenic chromosomal alterations (9).

A hallmark of cancer is that sustained expression or activity of oncogenic lesions are necessary to maintain the malignant state, and this especially applies to tumors driven by Myc, wherein even rather brief inactivation of Myc usually leads to complete tumor regression (12, 13). Thus, targeting Myc directly (e.g., blocking its transcription or translation or augmenting its turnover) could be therapeutic, yet Myc oncoproteins are also required for the growth of most normal cell types (14, 15), raising concerns of acquiring a suitable therapeutic index. Furthermore, the complexity of Myc's transcriptional response raises questions regarding which targets downstream of Myc to choose and whether intervention through any single target will show efficacy.

Ornithine decarboxylase (Odc), the first and a rate-limiting enzyme in the polyamine biosynthesis pathway, is a well-characterized, direct Myc transcription target (16, 17) clearly amenable to therapeutic intervention. Odc converts ornithine into putrescine, which is then converted into the more abundant polyamines spermidine and spermine (Supplementary Fig. S1), which control various aspects of cell biology, including replication, translation, and cell growth and survival (18, 19). Accordingly, polyamine levels are tightly maintained in cells, and these controls include the catabolic arm of the pathway that allows for back conversion (Supplementary Fig. S1) and, for Odc, also include regulation of its translation and turnover, which is directed by a dedicated inhibitor, coined antizyme, that directly shuttles Odc to the proteasome for destruction. In turn, an Odc decoy, coined antizyme inhibitor, dampens antizyme activity (reviewed in ref. 19).

Elevated Odc levels and accompanying increases in polyamine pools are common in cancer (18), and enforced Odc expression in the skin of transgenic mice leads to increased tumor incidence and rate in response to chemical carcinogens (20, 21). Furthermore, like Myc, Odc cooperates with activated Ras in transformation *in vitro* and *in vivo* (22, 23). Notably, *Odc* heterozygosity or treatment with the difluoromethylornithine (DFMO), a suicide inhibitor of Odc, impairs Myc-induced lymphomagenesis in Eμ-*Myc* transgenic mice

**Note:** Supplementary data for this article are available at Cancer Research Online (http://cancerres.aacrjournals.org/).

**Requests for reprints:** John L. Cleveland, Department of Cancer Biology, The Scripps Research Institute, Scripps Florida, 5353 Parkside Drive, RE-1, Jupiter, FL 33458. Phone: 561-799-8775; Fax: 561-799-8957; E-mail: jcleve@scripps.edu.



doi:10.1158/0008-5472.CAN-08-2968

(24), a model of human B-cell lymphoma (8). In B cells, targeting Odc selectively impairs the proliferative response of Myc by disabling its ability to suppress the expression of the cyclin-dependent kinase (Cdk) inhibitor $p27^{Kip1}$ (24). Importantly, recent clinical trials of colon and prostate cancer, two malignancies with known Myc involvement (e.g., ref. 11), have shown remarkable efficacy of DFMO as a chemoprevention agent (25, 26). Here, we tested the hypothesis that targeting Odc would also show efficacy in *MYCN*-driven neuroblastoma and report that DFMO, but not *Odc* heterozygosity, impairs the proliferative response of N-Myc and delays tumor incidence and onset. Interestingly, targeting Odc in this context affects the expression of a second arbiter of the proliferative response of Myc, the Cdk inhibitor $p21^{Cip1}$. Thus, targeting Odc disables Myc-induced tumorigenesis via distinct effectors, depending upon tumor type, yet this typically involves Cdk inhibitors that disable the proliferative response of Myc.

## Materials and Methods

**Array analyses.** The GSE3960 Series Matrix File was downloaded from National Center for Biotechnology Information Gene Expression Omnibus database. This file summarizes the expression profiles of 101 primary human neuroblastoma using Affymetrix U95Av2 arrays (27). *Z* scores were used in GeneSpring 7.3 (GS) for hierarchical clustering and visualization of microarray data. *Z* scores were calculated by subtracting the average gene signal in all arrays from the signal for each gene and dividing the result by the SD of all measured signals. Pearson correlation similarity measures and average linkage clustering algorithms were used in GS for hierarchical clustering of samples, which segregated the two major tumor groups. GS was also used for Student's *t* test between the two tumor groups. Genes with *P* values of <0.05 were identified as those that were significantly differentially expressed between the two tumor groups.

**RNA preparation and analyses.** Tumors were collected from TH-*MYCN* mice (9) at the time of sacrifice and were snap frozen. An aliquot of each tumor was homogenized. RNA from tumor samples and cultured cells was prepared using the RNeasy kit (Qiagen). The iScript cDNA synthesis kit (Bio-Rad) and 1 μg of RNA were used to prepare cDNA for quantitative real-time PCR (qRT-PCR). qRT-PCR was performed with the iTaq SYBRGreen kit and an iCycler machine (Bio-Rad). Data analyses were performed with the ΔΔCt method, wherein *ubiquitin* served as the internal control.

To assess potential effects of DFMO on the turnover of $p21^{Cip1}$ mRNA in *MYCN*-amplified neuroblastoma, IMR-32 and CHP-134 cells were either mock-treated or DFMO-treated for 3 d. Actinomycin D (10 μg/mL) was then added, cells were harvested at specific intervals, RNA was isolated, and $p21^{Cip1}$ mRNA levels were determined by qRT-PCR. Expression was standardized to the expression of *ubiquitin*; experiments were performed in duplicate.

**Western blot analyses.** Cell culture lysates and homogenized tumor aliquots from TH-*MYCN* mice were disrupted in lysis buffer [50 mmol/L HEPES (pH 7.5), 150 mmol/L NaCl, 1 mmol/L EDTA, 2.5 mmol/L EGTA, and 0.1% Tween 20 with 1 mmol/L phenylmethylsulfonyl fluoride, 10 mmol/L β-glycerophosphate, 1 mmol/L NaF, 1 mmol/L $NaVO_4$, and complete mini tablet protease inhibitor (Roche)] by sonication, as described (24). For analyses of $p21^{Cip1}$ levels in neuroblastoma cell lines, nuclear extracts were prepared, as described by Andrews and Faller (28). Protein (40–50 μg/lane) was separated on 10% SDS-polyacrylamide gels, transferred to polyvinylidene difluoride membranes (Immobilon-P, Millipore), and blotted for antibodies specific for N-Myc (OP13, Calbiochem), ODC (from Dr. Lisa Shantz, Pennsylvania State University School of Medicine), $p21^{Cip1}$ (for mouse, sc-6246, Santa Cruz; for human, sc-397, Santa Cruz), $p27^{Kip1}$ (610242, BD Transduction Labs), p53 (for mouse, 1C12, Cell Signaling; for human, sc-6243, Santa Cruz), actin (AC-15, Sigma), and α-tubulin (B-5-1-2, Sigma).

**Cell culture.** Human neuroblastoma cell lines SK-N-MC, SK-N-SH, IMR-32, and CHP-134 were obtained from American Type Culture Collection (ATCC) and were maintained in RPMI 1640 (Life Technologies) with 10% fetal bovine serum, 1× L-glutamine, 1× MEM nonessential amino acids, and 1% penicillin/streptomycin at 37°C, 5% $CO_2$. Cells were harvested for protein and RNA analyses. For treatment with DFMO, cells were split at $2.5 \times 10^6$ into 15-cm plates for protein analyses and $4 \times 10^5$ into 6-cm plates for RNA and fluorescence-activated cell sorting (FACS) analyses 4 h before 5 mmol/L DFMO treatment. Cells were cultured in the presence of DFMO for 72 h and then harvested for protein, RNA, or FACS analyses. For growth curve analysis, $1 \times 10^5$ cells were plated into six-well plates 4 h before 5 mmol/L DFMO or mock treatment. Each day, three wells of mock-treated and three wells of DFMO-treated cells were individually collected and counted. Cells were counted using a Cellometer Auto T4 cell counter (Nexcelom Bioscience).

**Mice and tumor analyses.** Mice expressing the human *MYCN* gene under the control of the rat *tyrosine hydroxylase* promoter (TH-*MYCN*; ref. 9) were maintained on a 129x1/SvJ background. TH-*MYCN* littermates were given either water, water containing 1% DFMO from weaning (~21 d) to sacrifice, or water containing 1% DFMO from weaning to 120 d of age. TH-*MYCN* were also bred to $Odc^{+/-}$ mice (ref. 29; on a 94% 129x1/SvJ background) to generate TH-*MYCN*;$Odc^{+/+}$ and TH-*MYCN*;$Odc^{+/-}$ littermates (97% 129x1/SvJ background). Mice were monitored daily for illness and tumor development. Sick animals were sacrificed, and tumors were collected, snap frozen, and stored at −80°C.

**Flow cytometry.** Cell cycle analysis was performed by using the FITC BrdU flow kit (559619, BD Biosciences). DFMO-treated or mock-treated (72 h) cultured cells were incubated with 10 μmol/L BrdUrd for 30 min and collected by trypsinization. Cells were stained for BrdUrd incorporation and cell cycle, as previously described (24). Stained cells were analyzed using a BD FACSCanto II; doublets were excluded based on pulse width/height and separated based on FITC staining (BrdUrd incorporation) versus 7-AAD (cell cycle).

## Results

***MYCN*-amplified neuroblastomas express elevated levels of *ODC*.** High-risk, stage IV neuroblastoma is often accompanied by *MYCN* amplification (3, 4). To initially canvass the potential relationships of amplified *MYCN* in neuroblastoma with the polyamine pathway, we performed hierarchical clustering of microarray data of 101 primary human neuroblastomas from Gene Expression Omnibus Series GSE3960, wherein ~20% of the tumors are *MYCN*-amplified (27). Several polyamine biosynthetic genes were up-regulated in *MYCN*-amplified versus non–*MYCN*-amplified tumors, including *ODC, AMD1* (*S*-adenosylmethionine decarboxylase), *SMS* (spermidine synthase), and *SRM* (spermine synthase; Fig. 1*A*). In addition, there were significantly reduced levels of the ODC antagonist antizyme 2 (*OAZ2*) in *MYCN*-amplified neuroblastoma, whereas other components of the pathway were not significantly different between the two tumor cohorts (Fig. 1*A*). Collectively, these data suggest an increase in polyamine pools in *MYCN*-amplified neuroblastoma.

The expression of the entire polyamine pathway was also interrogated in the SK-N-MC, SK-N-SH, IMR-32, and CHP-134 human neuroblastoma cell lines. SK-N-MC and SK-N-SH are non–*MYCN*-amplified neuroblastoma cells, whereas IMR-32 and CHP-134 contain 25 and 100 copies of the *MYCN* gene per cell, respectively (30). qRT-PCR and Western blot analyses confirmed that IMR-32 and CHP-134 cells expressed much higher levels of *MYCN* RNA and protein than SK-N-MC and SK-N-SH cells (Fig. 1*B* and *C*). The levels of *ODC* were also increased in the *MYCN*-amplified cell lines, IMR-32 (1.8-fold) and CHP-134 (2.2-fold), compared with SK-N-MC (1.0-fold) and SK-N-SH cells (1.2-fold; Fig. 1*B*). Similarly, ODC protein levels were elevated in the *MYCN*-amplified versus non–*MYCN*-amplified neuroblastoma cell lines (Fig. 1*C*). Therefore, ODC expression is selectively elevated in

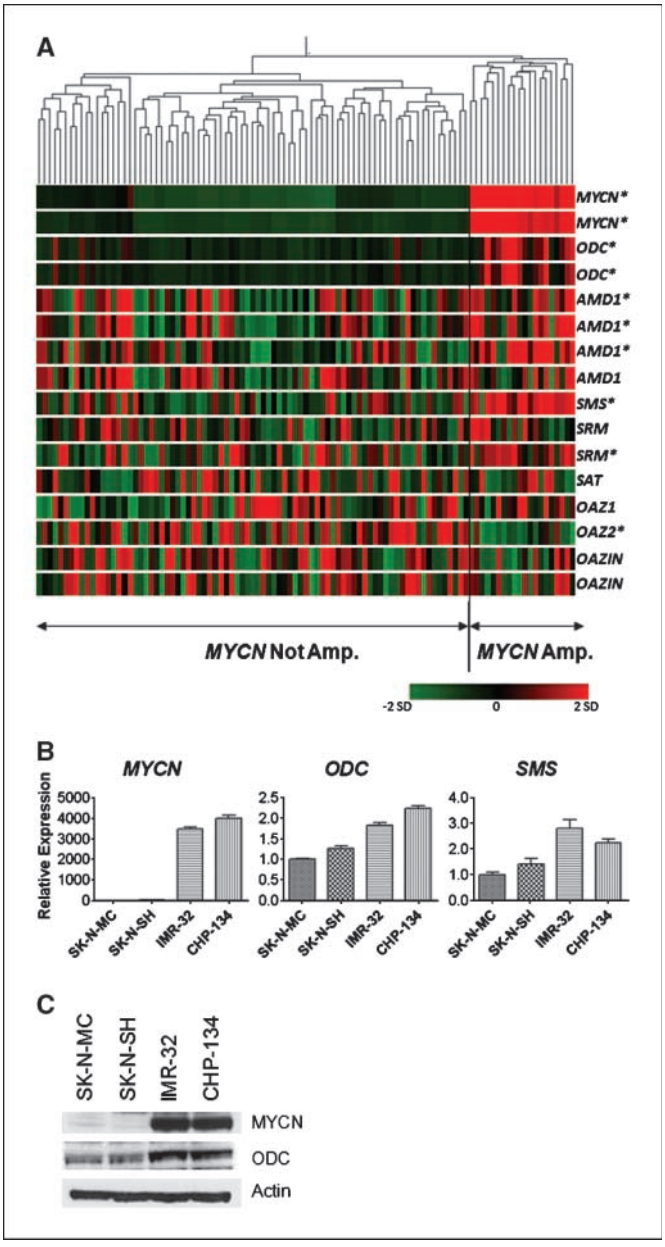


**Figure 1.** Pediatric neuroblastoma with *MYCN* amplification expresses elevated levels of ODC. *A,* hierarchical clustering of *MYCN*-amplified and nonamplified primary human neuroblastoma samples from Gene Expression Omnibus Series GSE3960. This clustering differentiated *MYCN*-expressing and nonexpressing tumors. Genes within the polyamine pathway present in the Affymetrix microarray data are shown. Genes that are marked with an asterisk (*) are significantly different ($P < 0.05$) between the *MYCN*-amplified and non–*MYCN*-amplified groups. *B,* real-time PCR analysis comparing the mRNA expression of *MYCN* and polyamine pathway genes *ODC* and *SMS* in human neuroblastoma cell lines SK-N-MC, SK-N-SH, IMR-32, and CHP-134. The relative expression level of each gene is set at 1.0 for the SK-N-MC cell line, and levels of mRNA are standardized to the expression of *ubiquitin*, which is not regulated by Myc oncoproteins. SE bars are provided for each cell line. The qRT-PCR analysis for other polyamine genes is provided in Supplementary Fig. S2. *C,* Western blot analysis of MYCN, ODC, and actin in human neuroblastoma cell lines SK-N-MC, SK-N-SH, IMR-32, and CHP-134.

*MYCN*-amplified primary neuroblastoma and neuroblastoma cell lines.

The expression levels of the other genes in the polyamine pathway were also assessed in these neuroblastoma cell lines by qRT-PCR. Here, although the expression of spermidine synthase was elevated in the *MYCN*-amplified lines (Fig. 1*B*), the expression of others that were significantly different in primary neuroblastoma were either unchanged between the two cell line cohorts (e.g., *AMD1* and *SSAT*) or were regulated in an inverse fashion (e.g., *SRM* and *OAZ2*; Supplementary Fig. S2). Thus, the expression of the ODC and SMS polyamine biosynthetic enzymes pathway are concordant between *MYCN*-amplified primary neuroblastoma and *MYCN*-amplified neuroblastoma cell lines.

**DFMO selectively impairs the proliferation of *MYCN*-amplified neuroblastoma.** The increased levels of ODC in *MYCN*-amplified neuroblastoma and *MYCN*-amplified neuroblastoma cell lines suggested that inhibiting ODC might selectively affect neuroblastoma with *MYCN* involvement. To test this notion, we initially assessed the effects of DFMO, an agent that was originally developed as a suicide inhibitor of the active ODC dimer (19), on the growth and/or survival of *MYCN*-amplified neuroblastoma cells. DFMO had no appreciable effects on the survival of any of the four neuroblastoma cell lines (data not shown). By contrast, DFMO had selective effects on the proliferation of *MYCN*-amplified versus non–*MYCN*-amplified neuroblastoma cell lines (Fig. 2*A*). Here, there were marked increases in the percentages of IMR-32 and CHP134 cells in $G_1$ and corresponding reductions in the percentage of these cells in S phase (Fig. 2*A* and Supplementary

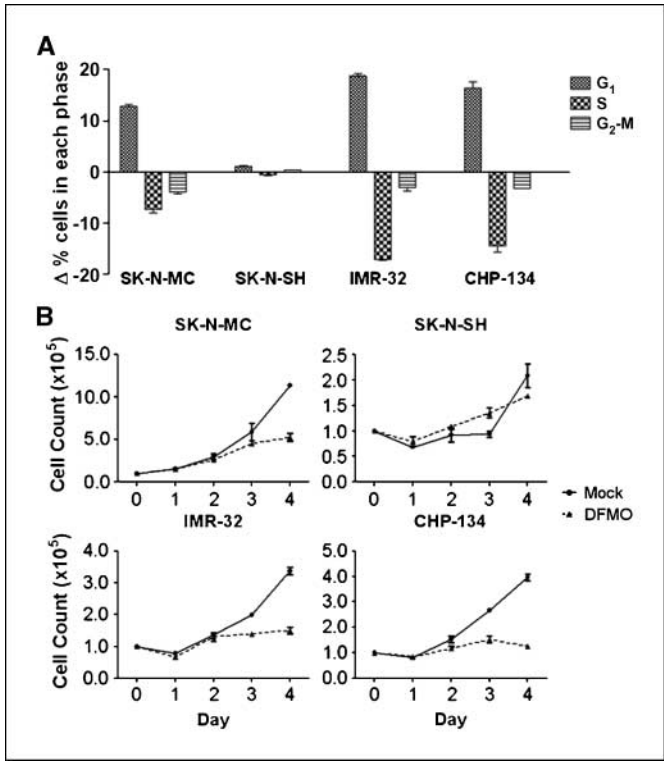


**Figure 2.** DFMO selectively impairs the proliferation of *MYCN*-amplified human neuroblastoma. *A,* the change in cell cycle distribution of the human neuroblastoma cell lines SK-N-MC, SK-N-SH, IMR-32, and CHP-134 upon DFMO treatment for 72 h. Cells were labeled with BrdUrd, harvested, and analyzed by FACS. The graph represents the difference in the average of two mock-treated samples and two DFMO-treated samples for each cell line (see also Supplementary Fig. S3). *B,* human neuroblastoma cell lines SK-N-MC, SK-N-SH, IMR-32, and CHP-134 were either mock-treated (*solid line*) or were treated with DFMO (5 mmol/L, *dashed lines*), and cell number was determined daily. The graph shown represents the average cell count relative for three mock-treated samples and three DFMO-treated samples from each cell line. SE bars are provided.

Fig. S3). By contrast, DFMO had only modest effects on the proliferation of SK-N-MC cells and had no effect on the growth of SK-N-SH cells (Fig. 2*A* and Supplementary Fig. S3). Accordingly, growth curve experiments ± DFMO showed that DFMO treatment effectively abolished the growth of *MYCN*-amplified IMR-32 and CHP-134 neuroblastoma cells but had more modest effects on the rates of cell growth of SK-N-MC cells and none whatsoever on SK-N-SH cells (Fig. 2*B*). Therefore, the growth of *MYCN*-amplified neuroblastoma cells is dependent upon ODC.

**DFMO, but not *Odc* heterozygosity, impairs N-Myc–driven neuroblastoma.** In Eμ-*Myc* transgenic mice, either DFMO or *Odc* heterozygosity impairs the proliferative response of c-Myc in B cells and markedly delays lymphomagenesis (24). Given the selective effects of DFMO on the proliferation of *MYCN*-amplified neuroblastoma cells, we reasoned that similar responses would be manifest in the rat *tyrosine hydroxylase* promoter-driven TH-*MYCN* transgenic model, which overexpress N-Myc in the sympathetic nervous tissue derived from the neural crest and which develop neuroblastoma with ~70% penetrance. Notably, hemizygous TH-*MYCN* mice develop tumors that are histologically similar to those arising in pediatric stage IV, *MYCN*-amplified neuroblastoma, including syntenic gain and loss of chromosomes (9). Beginning at 3 weeks of age, these transgenic mice were treated with 1% DFMO in their drinking water, a dose that effectively blocks Odc enzyme activity *in vivo* and leads to marked reductions in putrescine and spermidine pools (24). These mice were then followed for neuroblastoma development and compared with the control transgenic cohort that received normal drinking water. As expected (31), 74% (20 of 27) of untreated TH-*MYCN* mice developed neuroblastoma by 1 year of age. By contrast, only 48% (12 of 25) of TH-*MYCN* mice receiving DFMO-drinking water developed neuroblastoma by 1 year of age (Fig. 3*A*). Furthermore, DFMO also delayed disease, wherein the median survival of the DFMO-treated cohort that developed neuroblastoma was 139 days and that of the untreated cohort was 84 days (Fig. 3*A*). Therefore, DFMO delays both the onset and the incidence of neuroblastoma.

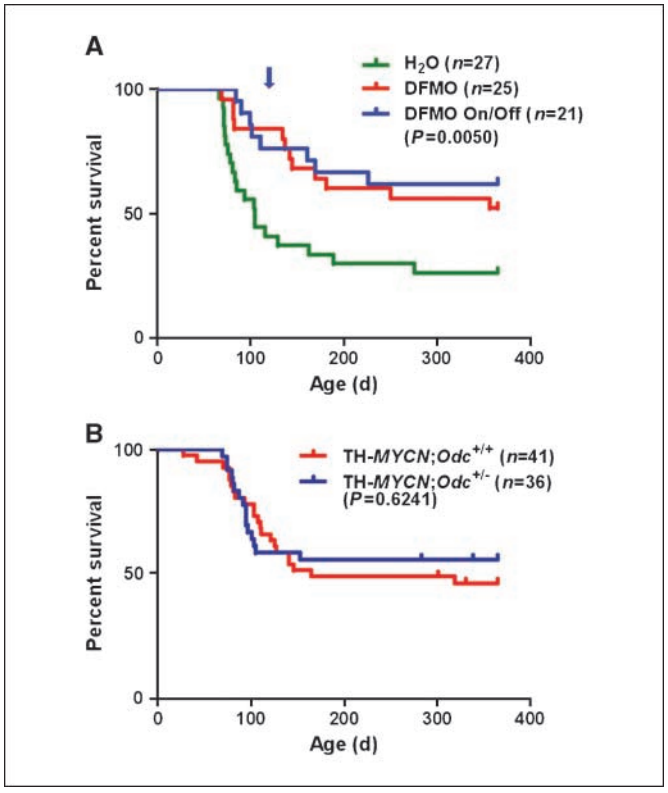


**Figure 3.** DFMO-treatment suppresses neuroblastoma development in TH-*MYCN* transgenic mice. *A,* survival curve of TH-*MYCN* transgenic mice untreated ($H_2O$), DFMO-treated, or DFMO-treated from weaning until 120 d of age. The blue arrow above the graph indicates the time (120 d of age) when a cohort of DFMO-treated mice was taken off the drug. Comparison of the survival curves by the Mantel-Cox log-rank test shows that the curves are significantly different ($P$ = 0.0050). *B,* survival curve of TH-*MYCN*;*Odc*$^{+/+}$ mice versus TH-*MYCN*;*Odc*$^{+/-}$ littermates. Comparison of the survival curves by the Mantel-Cox log-rank test shows that the curves are not significantly different ($P$ = 0.6241).

In Eμ-*Myc* transgenics, continuous DFMO treatment is required to prevent lymphoma development, and when treated transgenics are deprived of the drug, they develop lymphoma with kinetics nearly identical to that of untreated Eμ-*Myc* mice (24). To address whether this was also the case for *MYCN*-driven neuroblastoma, a cohort of TH-*MYCN* mice received DFMO-treated water from 3 weeks of age until they were 120 days old, at which time they were then withdrawn from the drug. Surprisingly, only 38% (8 of 21) of this cohort of mice succumbed to disease (Fig. 3*A*). Thus, only transient exposure to DFMO is needed for chemoprevention, a finding which suggests that Odc activity is only required early during neuroblastoma development.

To test if *Odc* heterozygosity would similarly impair neuroblastoma development, we backcrossed *Odc*$^{+/-}$ mice on to a 129x1/SvJ background until they were ~94% 129x1/SvJ, and these mice were then crossed to TH-*MYCN* mice (129x1/SvJ) to generate TH-*MYCN*;*Odc*$^{+/+}$ and TH-*MYCN*; *Odc*$^{+/-}$ littermates (~97% 129x1/SvJ), which were followed for 1 year for neuroblastoma development. On this mixed background, incidence of disease was reduced to 54% (22 of 41) for the TH-*MYCN*;*Odc*$^{+/+}$ cohort. In this context, *Odc* heterozygosity did not significantly affect disease incidence ($P$ = 0.6241), wherein 44% (16 of 36) of TH-*MYCN*;*Odc*$^{+/-}$ mice developed neuroblastoma (Fig. 3*B*). Furthermore, there was no significant difference in the median survival between the two cohorts (Fig. 3*B*). Therefore, *Odc* heterozygosity is not sufficient to prevent Myc-driven cancer in this context. However, the reductions in penetrance of neuroblastoma from 74% on a pure 129x1/SvJ background (Fig. 3*A*), where disease penetrance and severity is most manifested (9), to that observed for TH-*MYCN*;*Odc*$^{+/+}$ mice (54% penetrance; Fig. 3*B*) could potentially mask modest effects of *Odc* heterozygosity on N-Myc–driven tumorigenesis.

**DFMO targets p21$^{Cip1}$ to impair the growth of *MYCN*-amplified neuroblastoma.** In Eμ-*Myc* B cells, targeting Odc disables Myc-mediated suppression of p27$^{Kip1}$ (24). We, therefore, tested whether DFMO-induced growth arrest in *MYCN*-amplified neuroblastoma cells was also specifically associated with increased levels of p27$^{KIP1}$. As expected, there were no effects of DFMO on the expression of N-MYC protein or *ODC* in *MYCN*-amplified neuroblastoma, but surprisingly, there were also no effects of DFMO on p27$^{KIP1}$ mRNA or protein levels (Fig. 4*A* and *B*). Myc also suppresses the transcription of the Cdk inhibitor p21$^{Cip1}$ (32, 33); thus, we tested whether DFMO disables this response in *MYCN*-amplified neuroblastoma. Indeed, qRT-PCR and Western blot analyses established that DFMO induced marked and selective increases in *p21$^{CIP1}$* mRNA levels in the IMR-32 and CHP-134 *MYCN*-amplified cell lines (Fig. 4*A*). *p21$^{CIP1}$* is a known transcription target of p53 (34) but *p21$^{CIP1}$* induction by DFMO was not associated with increased levels of p53 (Fig. 4*B*), which is wild type

in this cast of neuroblastoma cells (35).[1] However, the induction of *p21$^{CIP1}$* mRNA by DFMO did seem to be due to effects on transcription, as DFMO had no effects on the $t_{1/2}$ of *p21$^{CIP1}$* mRNA in actinomycin-D experiments, which measured their turnover (Supplementary Fig. S4). Importantly, the induction of p21$^{CIP1}$ by DFMO was also manifested at the protein level, wherein there were selective increases in p21$^{CIP1}$ protein in DFMO-treated IMR-32 and CHP-134 *MYCN*-amplified neuroblastoma (Fig. 4*B*). Therefore, the selective effects of DFMO in impairing the proliferative response of *MYCN*-amplified neuroblastoma are associated with increases in p21$^{CIP1}$ expression.

**DFMO targets p21$^{Cip1}$ in TH-*MYCN* neuroblastoma.** The findings that DFMO selectively targeted p21$^{CIP1}$ in human neuroblastoma suggested that this pathway would also be involved and targeted *in vivo* in neuroblastoma arising in TH-*MYCN* transgenics. One prediction was that p21$^{Cip1}$ expression would be generally suppressed in such TH-*MYCN* tumors. Indeed, only 3 of 11 neuroblastomas from TH-MYCN transgenics showed detectable levels of p21$^{Cip1}$ protein (Fig. 5*A*). In contrast, nearly all neuroblastoma expressed p27$^{Kip1}$ (Fig. 5*A*) and again in contrast to Myc-driven lymphomas where p27$^{Kip1}$ protein levels are suppressed (24). Therefore, p21$^{Cip1}$ expression is suppressed in N-Myc–driven neuroblastoma.

A second prediction was that DFMO treatment would selectively affect p21$^{Cip1}$ expression in the delayed-onset tumors that eventually arose in the DFMO-treated cohort of TH-MYCN mice. Indeed, levels of *p21$^{Cip1}$* mRNA and protein were higher in most DFMO-treated tumors compared with the untreated cohort (Fig. 5*A* and *B*). Therefore, DFMO also induces the expression of *p21$^{Cip1}$* in *MYCN*-driven neuroblastoma *in vivo*. In contrast, levels of *MYCN* RNA and protein and of *p27$^{Kip1}$* were unaffected by DFMO (Fig. 5*A* and *B*).

*ODC* amplification has been described as a mechanism of DFMO resistance (36); thus, we also assessed whether Odc was induced in the DFMO-treated cohort. Indeed, there were marked increases in Odc protein in the DFMO-treated cohort of neuroblastoma (Fig. 5*A*). However, the *Odc* gene was not amplified in these tumors (Supplementary Fig. S5) and levels of *Odc* transcripts were similar between the two cohorts (Fig. 5*B*). Therefore, up-regulation of Odc in the DFMO-treated cohort seems due to either alterations in Odc translation or turnover.

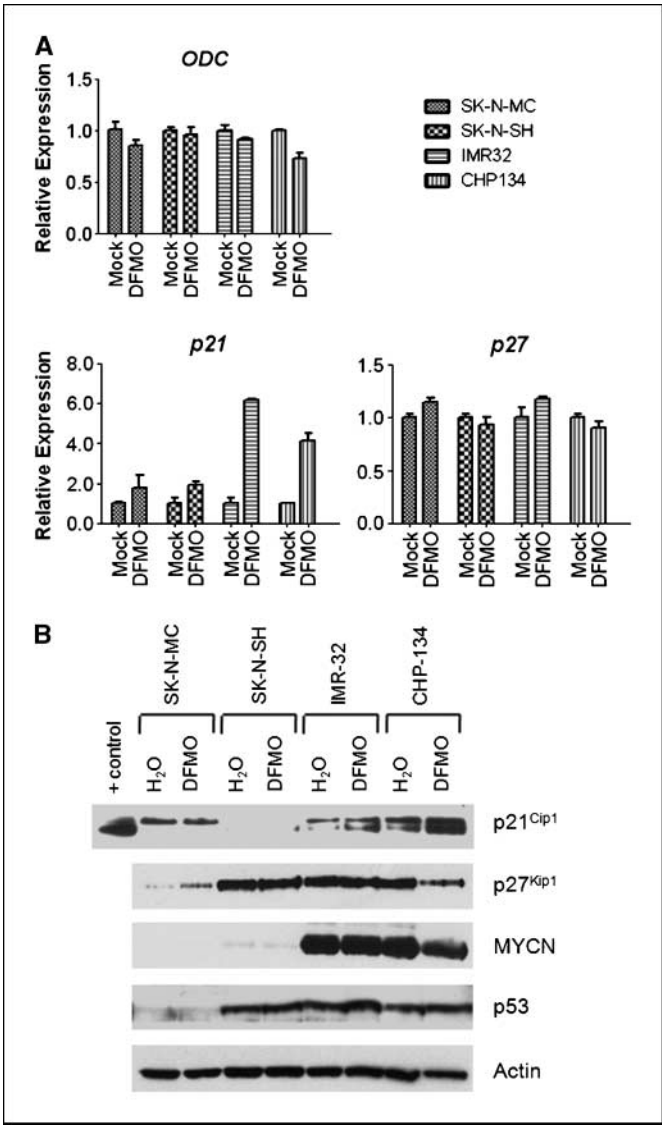


**Figure 4.** DFMO-induced growth arrest of *MYCN*-amplified neuroblastoma is associated with the selective induction of p21$^{Cip1}$. *A,* qRT-PCR analysis comparing the *ODC, p21$^{CIP1}$*, and *p27$^{KIP1}$* mRNA levels in human neuroblastoma cell lines SK-N-MC, SK-N-SH, IMR-32, and CHP-134 after DFMO treatment for 72 h. The graph represents the average relative expression for two mock-treated samples and two DFMO-treated samples from each cell line. The relative expression level of each gene is set at 1.0 for the mock-treated samples of each cell line, and levels of mRNA are standardized to the expression of *ubiquitin*, which is not regulated by Myc oncoproteins. SE bars are provided for each cell line. *B,* Western blot analysis of MYCN, p21$^{Cip1}$, p27$^{Kip1}$, p53, and actin in human neuroblastoma cell lines SK-N-MC, SK-N-SH, IMR-32, and CHP-134, either mock-treated or DFMO-treated for 72 h.

## Discussion

Myc oncoproteins augment the rate of cell proliferation (37), and in Eμ-*Myc* transgenic mice this response is limiting for tumor onset and survival. Specifically, in B cells enforced c-Myc expression increases the number of cells in cycle by repressing p27$^{Kip1}$ protein levels, and this occurs through the Myc-mediated regulation of E2f1 and Cks1, which together are required for activating the SCF$^{SKP2}$ complex that targets p27$^{Kip1}$ for destruction by the proteasome (38, 39). Accordingly, loss of *p27$^{Kip1}$* accelerates rates of Myc-induced lymphoma development (40), whereas loss of either *E2f1* or *Cks1* compromises Myc's proliferative response, suppression of p27$^{Kip1}$, and onset and incidence of Myc-drive lymphoma (38, 39). Quite strikingly, the Myc-to-p27$^{Kip1}$ pathway is also controlled by the polyamine pathway, wherein Odc expression is greatly elevated in Eμ-*Myc* B cells and targeting Odc with DFMO or *Odc* heterozygosity blocks the ability of Myc to repress p27$^{Kip1}$ (24).

The findings presented herein show some parallels of targeting Odc in *MYCN*-amplified neuroblastoma compared with Myc-overexpressing B cells. Specifically, akin to Myc-driven B-cell lymphomas of mice and man, *ODC* is also overexpressed in stage IV, *MYCN*-amplified pediatric neuroblastoma, findings consistent with *ODC* being a direct transcription target of Myc oncoproteins (16, 17). Furthermore, DFMO also selectively cancels the proliferative response of *MYCN*-amplified neuroblastoma and dramatically impairs the onset and incidence of N-Myc–driven neuroblastoma *in vivo*. However, interesting and

[1] http://www.sanger.ac.uk/genetics/CGP/CellLines/

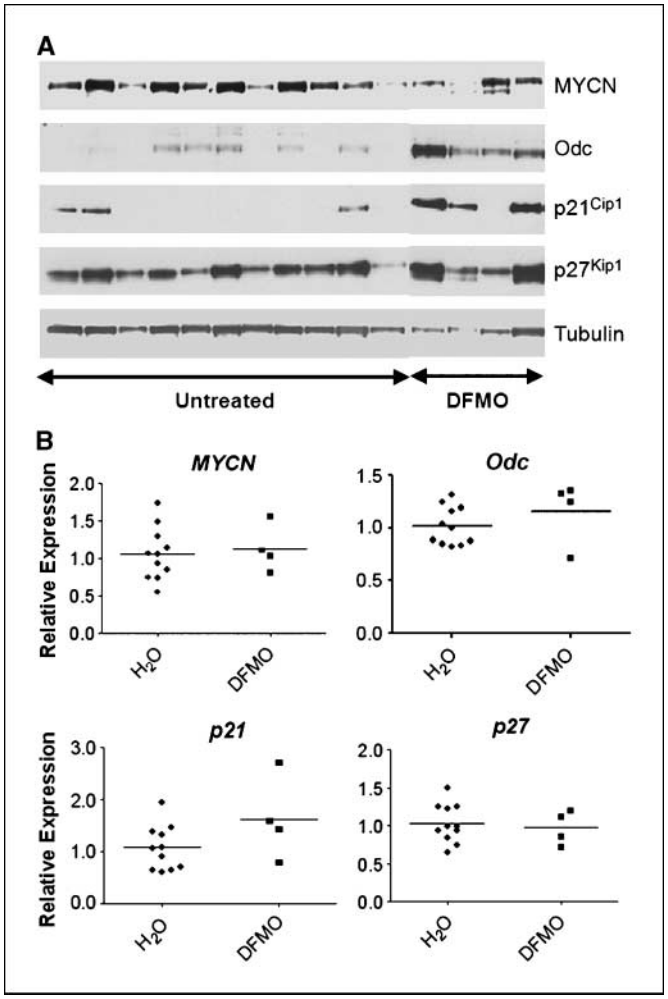


**Figure 5.** Neuroblastomas that develop in DFMO-treated TH-*MYCN* mice have elevated levels of $p21^{Cip1}$. *A,* Western blot analysis of MYCN, ODC, $p21^{Cip1}$, $p27^{Kip1}$, and tubulin levels in individual neuroblastoma arising in untreated or DFMO-treated TH-*MYCN* transgenic mice. *B,* qRT-PCR analysis comparing the levels of *MYCN, ODC,* $p21^{Cip1}$, and $p27^{Kip1}$ mRNAs in neuroblastoma that arose in either untreated ($H_2O$) or DFMO-treated TH-*MYCN* transgenic mice. The relative expression in individual tumor samples is indicated by the individual marks (*circle,* untreated; *squares,* DFMO-treated) on the scatter blot, and the average relative expression for the group is indicated by the bar. The average relative expression level of each gene is set at 1.0 for the untreated group, and levels of mRNA are standardized to the expression of *ubiquitin*, which is not regulated by N-Myc. qRT-PCR analysis shows that the expression of other genes in the polyamine pathway was unaffected in the DFMO-treated cohort of neuroblastoma (Supplementary Fig. S6).

context-specific differences are also evident, wherein DFMO effects on the proliferative response driven by N-Myc are linked to effects on $p21^{Cip1}$ in both human and mouse neuroblastoma and only transient treatment with DFMO is necessary to achieve chemoprevention. Furthermore, *Odc* heterozygosity has no effect on tumorigenesis in this tumor model, whereas in Eμ-*Myc* transgenics and in carcinogen-driven papillomas, *Odc* heterozygosity has marked effects on tumor onset, incidence, and overall survival (24, 41). Cell type and/or tumor context-specific control of polyamine homeostasis could account for these differences and allow neural crest progenitors to overcome effects of reductions in *Odc*. Indeed, polyamine homeostasis is different between Myc-driven lymphoma and neuroblastoma, as all of the biosynthetic enzymes are up-regulated in Myc-induced B-cell lymphoma (24) whereas only *ODC* and *spermidine synthase* are increased in *MYCN*-amplified neuroblastoma (Fig. 1*A* and *B* and Supplementary Fig. S2). Finally, in neural crest progenitors, there may be no substantial effects of loss of one *Odc* allele on overall levels of Odc protein, on Odc enzyme activity, and/or on polyamine pools.

Loss of the neurofibromatosis-1 (Nf1) or retinoblastoma (Rb) tumor suppressors accelerates disease in TH-*MYCN* mice (9). These studies are consistent with apparent alterations of *NF1* in pediatric *MYCN*-amplified neuroblastoma (42, 43) and with the reduced expression of $p21^{Cip1}$ in most TH-*MYCN* neuroblastomas (Fig. 5), which express hyperphosphorylated (i.e., inactive) pRb (data not shown). They are also consistent with reduced $p21^{CIP1}$ expression in *MYCN*-amplified versus nonamplified human neuroblastoma ($P < 0.005$, Gene Expression Omnibus Series GSE3960; data not shown). They also underscore the unique genetics of this peculiar malignancy versus those driven by Myc in other scenarios, wherein there seems to be little to no contribution of $p21^{Cip1}$ on tumor development (40). Finally, these findings support the interesting notion that Myc activation in different tumor types selects for the inactivation of distinct tumor suppressor pathways, which contribute to malignant progression.

The mechanisms by which targeting Odc induces the $p27^{Kip1}$ and $p21^{Cip1}$ inhibitors to impair the proliferative response of Myc in lymphoma versus neuroblastoma, respectively, are not fully understood. In B cells, targeting Odc disables the ability of Myc to trigger $p27^{Kip1}$ protein degradation, and here, effects appear via Cks1,[2] which is induced by Myc and is a required component of the $SCF^{Skp2}$ complex that directs $p27^{Kip1}$ destruction (39, 44). By contrast, in *MYCN*-amplified neuroblastoma there are elevated levels of ODC and low levels of $p21^{CIP1}$ mRNA and protein, and DFMO seems to cancel the ability of N-Myc to repress $p21^{Cip1}$ transcription, both *ex vivo* and *in vivo*. We propose that *MYCN*-amplified cells are, similar to Myc-expressing B cells, "addicted" to ODC for their proliferative response and that, in neuroblastoma, this hinges upon proper regulation of $p21^{CIP1}$. Furthermore, we suspect that the effects of DFMO on $p21^{Cip1}$ expression that have been observed in some tumor cell lines (45, 46) reflect Myc involvement in the tumors from which they were derived, which renders these cells addicted to ODC. How DFMO may affect $p21^{CIP1}$ transcription in *MYCN*-amplified neuroblastoma is not yet clear. However, because this response seems to be p53-independent and does not involve changes in the $t_{1/2}$ of $p21^{CIP1}$ mRNA, we hypothesize that DFMO somehow interferes with Myc-mediated transcriptional repression of $p21^{CIP1}$, which occurs by binding of Myc to Miz-1 (32).

The findings that DFMO is an effective prevention agent in neuroblastoma were quite surprising, because the *tyrosine hydroxylase* promoter driving the *MYCN* transgene is active from the genesis of the neural crest early in development. Thus, one would predict more benefit if DFMO was given earlier in life. However, DFMO cannot be given during gestation, where this drug or total loss of *Odc* causes early embryonic lethality (37, 47), nor after birth, as there are side effects on neuronal development (48). Thus, there are valid concerns whether DFMO could be given in a safe manner to pediatric patients suffering from stage IV *MYCN*-amplified neuroblastoma. Nonetheless, with the low doses of DFMO that

[2] J.L. Cleveland, unpublished data.

have been given in the colon and prostate cancer chemoprevention trials, wherein there were no noticeable side effects (25, 26), it may be wise to revisit this issue for stage IV neuroblastoma because transient treatment with DFMO here is also sufficient to provide chemoprevention and especially because it may show benefit for this otherwise lethal malignancy. Notably, recent findings that *ODC* overexpression is a superior indicator of poor prognosis in neuroblastoma (49) suggests that even those patients lacking *MYCN* amplicons but overexpressing ODC may experience benefit from DFMO treatment. Regardless, our studies do suggest that targeting the polyamine pathway should perhaps be considered in combination with more conventional agents to treat this devastating disease.

## Disclosure of Potential Conflicts of Interest

No potential conflicts of interest were disclosed.

## Acknowledgments

Received 8/5/2008; revised 10/14/2008; accepted 10/22/2008.

**Grant support:** NIH grants R01-CA100603 (J.L. Cleveland) and F32-CA115075 (R.J. Rounbehler) and monies from State of Florida to the Scripps Research Institute.

The costs of publication of this article were defrayed in part by the payment of page charges. This article must therefore be hereby marked *advertisement* in accordance with 18 U.S.C. Section 1734 solely to indicate this fact.

We thank the Animal Resource Center of Scripps-Florida for their assistance, Dr. William Weiss for providing the TH-*MYCN* transgenic mice, Dr. Lisa Shantz for the kind gift of the anti-ODC antibody, Dr. Meredith Steeves for assistance with generating the *Odc* Southern blot probe, and members of the Cleveland laboratory for their help and review.

## References

**1.** Cancer Incidence and Survival among Children and Adolescents: United States SEER Program, 1975-1995. In: Ries LAG, Smith MA, Gurney JG, Linet M, Tamra T, Young JL, Bunin GR, editors. National Cancer Institute, SEER Program; 1999.

**2.** De Bernardi B, Nicolas B, Boni L, et al. Disseminated neuroblastoma in children older than one year at diagnosis: comparable results with three consecutive high-dose protocols adopted by the Italian Co-operative Group for Neuroblastoma. J Clin Oncol 2003;21:1592–601.

**3.** Seeger RC, Brodeur GM, Sather H, et al. Association of multiple copies of the N-myc oncogene with rapid progression of neuroblastomas. N Engl J Med 1985;313:1111–6.

**4.** Brodeur GM, Seeger RC, Schwab M, Varmus HE, Bishop JM. Amplification of N-myc in untreated human neuroblastomas correlates with advanced disease stage. Science 1984;224:1121–4.

**5.** Lee LA, Dang CV. Myc target transcriptomes. Curr Top Microbiol Immunol 2006;302:145–67.

**6.** Fernandez PC, Frank SR, Wang L, et al. Genomic targets of the human c-Myc protein. Genes Dev 2003;17:1115–29.

**7.** Orian A, van Steensel B, Delrow J, et al. Genomic binding by the *Drosophila* Myc, Max, Mad/Mnt transcription factor network. Genes Dev 2003;17:1101–14.

**8.** Adams JM, Harris AW, Pinkert CA, et al. The c-myc oncogene driven by immunoglobulin enhancers induces lymphoid malignancy in transgenic mice. Nature 1985;318:533–8.

**9.** Weiss WA, Aldape K, Mohapatra G, Feuerstein BG, Bishop JM. Targeted expression of MYCN causes neuroblastoma in transgenic mice. EMBO J 1997;16:2985–95.

**10.** D'Cruz CM, Gunther EJ, Boxer RB, et al. c-MYC induces mammary tumorigenesis by means of a preferred pathway involving spontaneous Kras2 mutations. Nat Med 2001;7:235–9.

**11.** Ellwood-Yen K, Graeber TG, Wongvipat J, et al. Myc-driven murine prostate cancer shares molecular features with human prostate tumors. Cancer Cell 2003;4:223–38.

**12.** Felsher DW, Bishop JM. Reversible tumorigenesis by MYC in hematopoietic lineages. Mol Cell 1999;4:199–207.

**13.** Jain M, Arvanitis C, Chu K, et al. Sustained loss of a neoplastic phenotype by brief inactivation of MYC. Science 2002;297:102–4.

**14.** de Alboran IM, O'Hagan RC, Gartner F, et al. Analysis of C-MYC function in normal cells via conditional gene-targeted mutation. Immunity 2001;14:45–55.

**15.** Trumpp A, Refaeli Y, Oskarsson T, et al. c-Myc regulates mammalian body size by controlling cell number but not cell size. Nature 2001;414:768–73.

**16.** Bello-Fernandez C, Packham G, Cleveland JL. The ornithine decarboxylase gene is a transcriptional target of c-Myc. Proc Natl Acad Sci U S A 1993;90:7804–8.

**17.** Wagner AJ, Meyers C, Laimins LA, Hay N. c-Myc induces the expression and activity of ornithine decarboxylase. Cell Growth Differ 1993;4:879–83.

**18.** Gerner EW, Meyskens FL, Jr. Polyamines and cancer: old molecules, new understanding. Nat Rev Cancer 2004;4:781–92.

**19.** Pegg AE. Regulation of ornithine decarboxylase. J Biol Chem 2006;281:14529–32.

**20.** O'Brien TG, Megosh LC, Gilliard G, Soler AP. Ornithine decarboxylase overexpression is a sufficient condition for tumor promotion in mouse skin. Cancer Res 1997;57:2630–7.

**21.** Chen Y, Megosh LC, Gilmour SK, Sawicki JA, O'Brien TG. K6/ODC transgenic mice as a sensitive model for carcinogen identification. Toxicol Lett 2000;116:27–35.

**22.** Hibshoosh H, Johnson M, Weinstein IB. Effects of overexpression of ornithine decarboxylase (ODC) on growth control and oncogene-induced cell transformation. Oncogene 1991;6:739–43.

**23.** Smith MK, Trempus CS, Gilmour SK. Co-operation between follicular ornithine decarboxylase and v-Ha-ras induces spontaneous papillomas and malignant conversion in transgenic skin. Carcinogenesis 1998;19:1409–15.

**24.** Nilsson JA, Keller UB, Baudino TA, et al. Targeting ornithine decarboxylase in Myc-induced lymphomagenesis prevents tumor formation. Cancer Cell 2005;7:433–44.

**25.** Simoneau AR, Gerner EW, Nagle R, et al. The effect of difluoromethylornithine on decreasing prostate size and polyamines in men: results of a year-long phase IIb randomized placebo-controlled chemoprevention trial. Cancer Epidemiol Biomarkers Prev 2008;17:292–9.

**26.** Meyskens FL, Jr., McLaren CE, Pelot D, et al. Difluoromethylornithine plus sulindac for the prevention of sporadic colorectal adenomas: a randomized placebo-controlled, double-blind trial. Cancer Prev Res 2008;1:32–8.

**27.** Wang Q, Diskin S, Rappaport E, et al. Integrative genomics identifies distinct molecular classes of neuroblastoma and shows that multiple genes are targeted by regional alterations in DNA copy number. Cancer Res 2006;66:6050–62.

**28.** Andrews NC, Faller DV. A rapid micropreparation technique for extraction of DNA-binding proteins from limiting numbers of mammalian cells. Nucleic Acids Res 1991;19:2499.

**29.** Pendeville H, Carpino N, Marine JC, et al. The ornithine decarboxylase gene is essential for cell survival during early murine development. Mol Cell Biol 2001;21:6549–58.

**30.** Reynolds CP, Tomayko MM, Donner L, et al. Biological classification of cell lines derived from human extra-cranial neural tumors. Prog Clin Biol Res 1988;271:291–306.

**31.** Chesler L, Goldenberg DD, Seales IT, et al. Malignant progression and blockade of angiogenesis in a murine transgenic model of neuroblastoma. Cancer Res 2007;67:9435–42.

**32.** Herold S, Wanzel M, Beuger V, et al. Negative regulation of the mammalian UV response by Myc through association with Miz-1. Mol Cell 2002;10:509–21.

**33.** Seoane J, Le HV, Massague J. Myc suppression of the p21(Cip1) Cdk inhibitor influences the outcome of the p53 response to DNA damage. Nature 2002;419:729–34.

**34.** el-Deiry WS, Tokino T, Velculescu VE, et al. WAF1, a potential mediator of p53 tumor suppression. Cell 1993;75:817–25.

**35.** Van Maerken T, Speleman F, Vermeulen J, et al. Small-molecule MDM2 antagonists as a new therapy concept for neuroblastoma. Cancer Res 2006;66:9646–55.

**36.** Leinonen P, Alhonen-Hongisto L, Laine R, Janne OA, Janne J. Human myeloma cells acquire resistance to difluoromethylornithine by amplification of ornithine decarboxylase gene. Biochem J 1987;242:199–203.

**37.** Roussel MF, Cleveland JL, Shurtleff SA, Sherr CJ. Myc rescue of a mutant CSF-1 receptor impaired in mitogenic signalling. Nature 1991;353:361–3.

**38.** Baudino TA, Maclean KH, Brennan J, et al. Myc-mediated proliferation and lymphomagenesis, but not apoptosis, are compromised by E2f1 loss. Mol Cell 2003;11:905–14.

**39.** Keller UB, Old JB, Dorsey FC, et al. Myc targets Cks1 to provoke the suppression of p27Kip1, proliferation and lymphomagenesis. EMBO J 2007;26:2562–74.

**40.** Martins CP, Berns A. Loss of p27(Kip1) but not p21(Cip1) decreases survival and synergizes with MYC in murine lymphomagenesis. EMBO J 2002;21:3739–48.

**41.** Guo Y, Cleveland JL, O'Brien TG. Haploinsufficiency for Odc modifies mouse skin tumor susceptibility. Cancer Res 2005;65:1146–9.

**42.** Johnson MR, Look AT, DeClue JE, Valentine MB, Lowy DR. Inactivation of the NF1 gene in human melanoma and neuroblastoma cell lines without impaired regulation of GTP-Ras. Proc Natl Acad Sci U S A 1993;90:5539–43.

**43.** The I, Murthy AE, Hannigan GE, et al. Neurofibromatosis type 1 gene mutations in neuroblastoma. Nat Genet 1993;3:62–6.

**44.** Pagano M, Tam SW, Theodoras AM, et al. Role of the ubiquitin-proteasome pathway in regulating abundance of the cyclin-dependent kinase inhibitor p27. Science 1995;269:682–5.

**45.** Ray RM, Zimmerman BJ, McCormack SA, Patel TB, Johnson LR. Polyamine depletion arrests cell cycle and induces inhibitors p21(Waf1/Cip1), p27(Kip1), and p53 in IEC-6 cells. Am J Physiol 1999;276:C684–91.

**46.** Kramer DL, Chang BD, Chen Y, et al. Polyamine depletion in human melanoma cells leads to G1 arrest associated with induction of p21WAF1/CIP1/SDI1, changes in the expression of p21-regulated genes, and a senescence-like phenotype. Cancer Res 2001;61:7754–62.

**47.** Fozard JR, Part ML, Prakash NJ, Grove J. Inhibition of murine embryonic development by α-difluoromethylornithine, an irreversible inhibitor of ornithine decarboxylase. Eur J Pharmacol 1980;65:379–91.

**48.** Sparapani M, Virgili M, Caprini M, Facchinetti F, Ciani E, Contestabile A. Effects of gestational or neonatal treatment with α-difluoromethylornithine on ornithine decarboxylase and polyamines in developing rat brain and on adult rat neurochemistry. Exp Brain Res 1996;108:433–40.

**49.** Haber M, Cheng N, Smith J, et al. Overexpression of ODC1 is associated with poor outcome in childhood neuroblastoma and represents an important therapeutic target [abstract #5832]. 99th AACR Annual Meeting; 2008.